Single-pulse ultrafast laser imprinting of axial dot arrays in bulk glasses

Cyril Mauclair, Alexandre Mermillod-Blondin, Landon Sébastien, Huot Nicolas, Arkadi Rosenfeld, Ingolf-Volker Hertel, Éric Audouard, I. Miyamoto, Razvan Stoian

Single pulse ultrafast laser imprinting of axial dot arrays in bulk glasses

C. Mauclair,[1,*] A. Mermillod-Blondin,[2] S. Landon,[1] N. Huot,[1] A. Rosenfeld,[2] I. V. Hertel,[2] E. Audouard,[1] I. Myiamoto,[3] and R. Stoian[1]

[1] *Laboratoire Hubert Curien (UMR 5516 CNRS), Université de Lyon, Université Jean Monnet, 42000 Saint Etienne, France*
[2] *Max-Born Institut für Nichtlineare Optik und Kurzzeitspektroskopie, D-12489 Berlin, Germany*
[3] *Osaka University, Osaka 565-0871, Japan*
[*] *Corresponding author: cyril.mauclair@univ-st-etienne.fr*

Compiled December 20, 2010

Ultrafast laser processing of bulk transparent materials can significantly gain in flexibility when the number of machining spots is increased. We present a new photoinscription regime where an array of regular dots is generated before the region of main laser focus under single pulse exposure in fused silica and borosilicate crown glass without any external spatial phase modulation. The specific position of the dots does not rely on nonlinear propagation effects but is mainly determined by beam truncation and is explained by a Fresnel propagation formalism taking into account beam apodization and linear wavefront distortions at the air/glass interface. The photoinscription regime is employed to generate a two-dimensional array of dots in fused silica. We show that an additional phase modulation renders flexible the pattern geometry.

OCIS codes: 000.0000, 999.9999.

Femtosecond laser sources are flexible tools for microprocessing of transparent materials [1]. When ultrashort laser pulses are focused inside a transparent material, the nonlinear interaction between the strong electromagnetic field and the dielectric material allows for localized modifications of the material structural properties. As a main result, the ultrafast exposure may modify several optical properties such as birefringence, absorption and refractive index on a micrometer scale [2]. The technique has reached an indisputable maturity with the fabrication of several embedded photonic devices (see [1] and references therein). There is a strong interest in improving the processing speed of the technique by multiplying the number of machining foci. With the help of wavefront tailoring devices such as spatial light modulators or diffractive optical elements, several groups have shown the possibility to increase the number of machined points for surface and bulk patterning [3, 4] and bulk parallel writing of waveguides [5]. As another solution to multipoint machining, the self-formation of regular voids under the accumulation of many light pulses was reported where the spacing, size and number of voids depend on the accumulation dose and the pulses energy [6, 7].

We present here a novel photoinscription regime allowing for single step multispot bulk writing without extrinsic user-induced wavefront manipulation and occurring with a single laser pulse. This results in the generation of regular micrometric modifications on the axis before the region of main focus with examples given here in fused silica (FS) and borosilicate crown glass (BK7).

Usually tightly focused femtosecond pulses confine severely the energy in the focal region [8]. However, it was demonstrated in particular conditions that the modified area can extend after the focus yielding consecutive voids with quite regular spacing. This regime usually requires a defined number of pulses and multiple refocusing points due to self-focusing or spherical aberrations [6, 7]. In this processing window, arrays of voxels were machined to illustrate of the applicative potential [7].

The photowriting regime we emphasize here has the significant advantage that only one light pulse suffices to generate tens of permanent dots without the need of spatial beam shaping systems. Fused silica and BK7 samples were irradiated with 160 fs pulses from an 800 nm Ti:Sapphire amplified ultrafast laser system operating at 160 Hz. Single pulses selected with a synchronized electromechanical shutter were focused inside the target by various microscope objectives with numerical apertures (NA) of 0.45, 0.42 and 0.28. The truncation ratio T is the ratio between the Gaussian beam diameter at the $1/e^2$ intensity point and the lens aperture diameter. We varied T from 0.5 to 1 in our calculations as well as experimentally using various magnifying telescopes before the focusing lens. The laser-induced structures were observed with a Zernike-type positive optical phase-contrast microscopy (PCM) system coupled to a high-resolution CCD camera providing a side-image of the relative changes in the refractive index induced by the irradiation. Positive and negative refractive index changes correspond to the image black and white areas, respectively. Figure 1 shows bulk modifications in FS and BK7 subsequent to single femtosecond pulse irradiation for various pulse energies. The laser focus is situated 200 μm beneath the material surface, in conditions of negligible spherical aberrations [9]. This location corresponds to the structures generated with the lowest pulse energy at the bottom of Fig.1 (a) and (b).

In the moderate energetic regimes below 2 μJ, we note a drastic difference in the response of BK7 and FS under laser irradiation as already reported [8]. While the response of BK7 is dominated by thermal expansion in a large region resulting in the onset of a low density material [10], the response of FS is characterized by the appearance of a reduced white zone in PCM correspond-

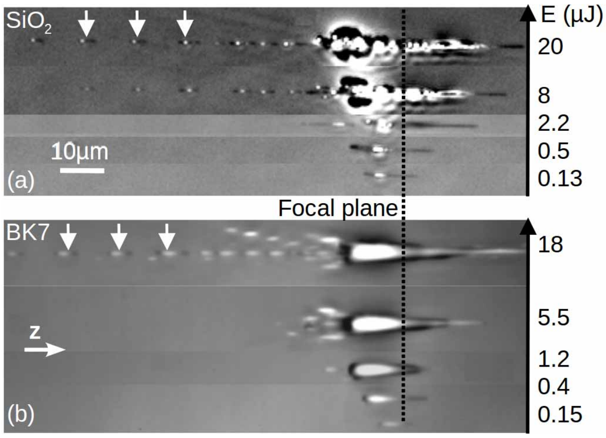

Fig. 1. PCM pictures of single pulse irradiation effects in FS and BK7 at different pulse energies (E) with NA= 0.45 and $T = 1$. The laser propagates along z. For sufficient energy, a particular photowriting regime occurs where regularly spaced dots appear up to 200 μm before the focus area upon single pulse in both glasses.

ing to a void [11], and a filament of higher refractive index. Time-resolved investigations associated the void with the region of stronger absorption of the electronic plasma and subsequent local mechanical rarefaction [12].

The new photoinscription regime is clearly observable on the traces obtained at the highest energies in Fig.1 and corresponds to powers (tens of MW) severly exceeding the critical power for self-focusing in both glasses. A very regular succession of dots (see arrows) aligned on the laser propagation axis z precedes the area of main focusing in both glasses. We observed that this line extends to the sample surface if sufficient pulse energy is employed, yielding ~ 20 dots under a single pulse. The local mapping of these pre-dots is quasi-identical in both materials which can be surprising since those glasses are known to behave very differently under femtosecond exposure [8]. In the context of femtosecond processing, it is tempting to assign the cartography of these structures to nonlinear propagation in the form of a regular succession of self-focusing and plasma defocusing phenomena, with repetitive concentration of light. In fact, it was shown that loose focusing conditions favoring filamentary propagation permit the photowriting of various permanent structures [13]. However a succession of self-focusing points strongly depends on the peak intensity and temporal characteristics of the pulse [14]. We conducted studies varying the pulse duration to validate this hypothesis (not shown). Investigations with longer pulses revealed that the position of the dots stays identical for pulse durations under the picosecond. For longer pulses, the dots do not appear. Also, comparing the 20 μJ and the 8 μJ irradiations in FS (Fig.1 (a)), shows that the position of the dots stays identical regardless of the pulse peak intensity, thus not validating the nonlinear propagation for being responsible for the dots mapping.

Interestingly, the distance separating two consecutive

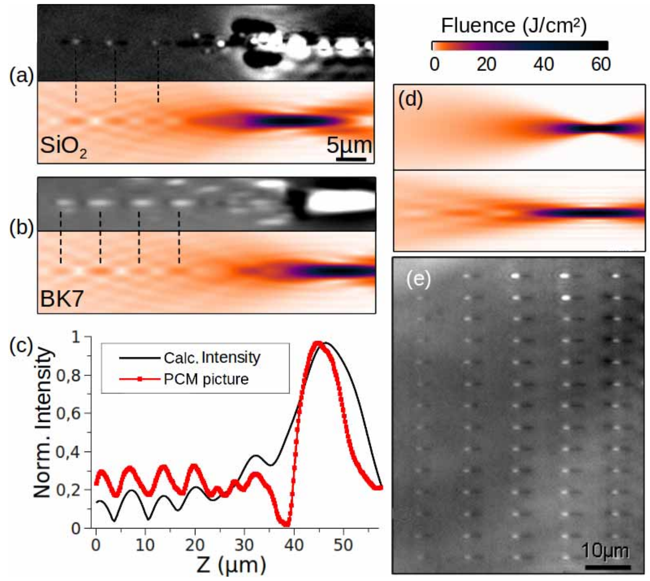

Fig. 2. (a), (b) PCM pictures of single pulse irradiation effects in FS and BK7 with the Fresnel propagation results with NA= 0.45 and $T = 1$. The dashed lines shows the correspondence between the position of the dots and the calculated fluence peaks. (c) Horizontal section of the PCM picture (red) and of the numerical results (black) for BK7. (d) Calculated focusing of a pure (top) and truncated (bottom) Gaussian beam showing fluence peaks before the focus due to truncation. (e) Array of dots written in FS in this regime. Each line was written with a single pulse. The main damage (not shown) is situated on the right.

dots is slightly smaller in FS than in BK7, following the tendency of their respective refractive indices at 800 nm ($n_{a-SiO_2} \approx 1.453$ and $n_{BK7} \approx 1.509$). This observation motivated us to precisely calculate the laser beam linear propagation using a Fresnel propagation code [15] to calculate the irradiation pattern over the focal volume. Within the paraxial approximation and neglecting spectral effects, the transverse intensity profile $I(x', y')$ after propagation over the distance D of a complex laser field $\tilde{A}(x, y)$ focused by a lens of focal distance f is defined by: $I(x', y') \propto \left| \mathcal{F}_{f_{x'}, f_{y'}} \left[\tilde{A}(x, y) e^{-\frac{i\pi}{\lambda}(x^2+y^2)\left(\frac{1}{D}-\frac{1}{f}\right)} \right] \right|^2$, where $\mathcal{F}_{f_{x'}, f_{y'}}$ is the two-dimensional (2D) Fourier Transform with respect to the spatial frequencies in the (x', y') plane. For a non-truncated collimated Gaussian beam, $\tilde{A}(x, y)$ reduces to a Gaussian function and the calculated fluence around the focus shows a single fluence peak at the beam waist (see Fig. 2 (d) top). The effect of beam truncation from the focusing lens can be incorporated in $\tilde{A}(x, y)$ with a rect function, resulting in a modulated fluence map with the appearance of fluence peaks before the main focus as illustrated in Fig. 2 (d) (bottom). We calculated the phase and amplitude of the laser beam after propagation from the lens until the air/glass interface. Then a phase term was added to

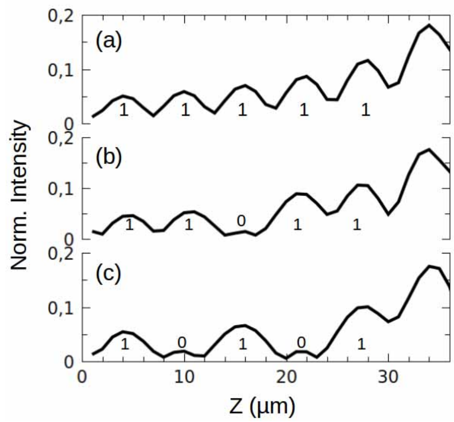

Fig. 3. Calculated intensity profiles along the optical axis z just before the main focus for different wavefront modulations controlling the dots local mapping. (a) no phase modulation yielding "11111" sequence. (b) and (c) various modulations yielding "11011" and "10101".

the laser spatial phase to take into account the phase distortion due to the refraction. The analytical expression of this additional phase term $\psi(\rho)$ is easily obtained from geometrical considerations [9].The air/glass interface is accompanied by a certain amount of reflection depending on the incidence angle and the beam polarization. We took into account the corresponding variation of amplitude using the corresponding Fresnel coefficients. The beam polarization is in the incidence plane which is parallel to the microscopy images shown here. The propagation calculations were then carried out for an ensemble of $X-Y$ planes comprising the focal area. Figure 2 (b) shows the calculated focal fluence maps for FS and BK7 with the PCM pictures of the bulk modification (respectively Fig. 2 (a) and (b)). The calculated fluence peaks preceding the focus precisely match the dots position (see the vertical dashed lines). An horizontal cross section along the optical axis of the PCM picture and the simulations is shown in Fig. 2 (c) for BK7. The mapping of the on-axis dots clearly matches the Fresnel propagation results. We also experimentally verified this correspondence for the other NAs (0.28 and 0.42). As a comparison, the non-truncated Gaussian propagation does not show the regular dot pattern (Fig.2 (d)). This was equally checked experimentally using $T = 0.5$ (not shown), validating thus the role of beam truncation.

As an illustration of the potential applications of this photowriting regime, a 2D array of dots is presented on Fig. 2 (e). The 70 shown dots were written with only 14 single pulse irradiations, which illustrates the possibility to write many structures with a high throughput. Those modifications can be used as data points or arrays of waveguides or phase gratings (i.e with a continuous irradiation under transversal displacement of the sample).

The next step is to show that the dots amplitude can be controlled to render this photowriting regime more appealing for data storage or multi-waveguide writing by higher flexibility. A phase-only spatial modulation appears as an appropriate way to achieve the dots position control while preserving a high energetic exposure. As an illustration of this potentiality, 2D phase modulations were numerically calculated with a evolutionary algorithm to produce user-defined dots mapping. Figure 3 shows the resulting numerical intensity profiles for three different optimized phase modulations showing the possibility to write arbitrary binary data sequences. The experimental implementation with a spatial phase modulators [5] will be the object of a future publication.

In conclusion, we described a novel single pulse photoinscription regime where an axial array of regular dots is generated before the main laser focus area in various glasses. The dots topology matches the fluence peaks calculated from Fresnel linear propagation simulations deriving essentially from the beam truncation. As an illustration, a 2D array of dots in FS is achieved in this processing window. An additional employement of spatial phase modulation increases the flexibility of the process leading to patterns at designed locations.

References

1. K. Itoh, W. Watanabe, S. Nolte, and C. B. Schaffer, MRS Bull **31**, 620 (2006).
2. E. Bricchi, B. G. Klappauf, and P. G. Kazansky, Opt. Lett. **29**, 119 (2004).
3. Y. Kuroiwa, N. Takeshima, Y. Narita, S. Tanaka, and K. Hirao, Opt. Express **12**, 1908 (2004).
4. S. Hasegawa, Y. Hayasaki, and N. Nishida, Opt. Lett. **31**, 1705 (2006).
5. C. Mauclair, G. Cheng, N. Huot, E. Audouard, A. Rosenfeld, I. V. Hertel, and R. Stoian, Opt. Express **17**, 3531 (2009).
6. J. Song, X. Wang, X. Hu, Y. Dai, J. Qiu, Y. Cheng, and Z. Xu, Appl. Phys. Lett. **92**, 092904 (2008).
7. S. Kanehira, J. Si, J. Qiu, K. Fujita, and K. Hirao, Nano Lett. **5**, 1591 (2005).
8. V. R. Bhardwaj, E. Simova, P. B. Corkum, D. M. Rayner, C. Hnatovsky, R. S. Taylor, B. Schreder, M. Kluge, and J. Zimmer, J. Appl. Phys. **97**, 083102 (2005).
9. N. Huot, R. Stoian, A. Mermillod-Blondin, C. Mauclair, and E. Audouard, Opt. Express **15**, 12395 (2007).
10. A. Mermillod-Blondin, I. M. Burakov, Yu. P. Meshcheryakov, N. M. Bulgakova, E. Audouard, A. Rosenfeld, A. Husakou, I. V. Hertel, and R. Stoian, Phys. Rev. B **77**, 104205 (2008).
11. E. N. Glezer and E. Mazur, Appl. Phys. Lett. **71**, 882 (1997).
12. A. Mermillod-Blondin, J. Bonse, A. Rosenfeld, I. V. Hertel, Y. P. Meshcheryakov, N. M. Bulgakova, E. Audouard, and R. Stoian, Appl. Phys. Lett. **94**, 041911 (2009).
13. K. Yamada, W. Watanabe, Y. Li, K. Itoh, and J. Nishii, Opt. Lett. **29**, 1846 (2004).
14. G. Heck, J. Sloss, and R. J. Levis, Opt. Commun. **259**, 216 (2006).
15. N. Huot, N. Sanner, and E. Audouard, J. Opt. Soc. Am. B **24**, 11 (2007).